Variability of Quiet-Time Magnetic Field Intensity Reconstructed from Spherical Harmonic Coefficients Over Asian-Sub Region

MUSTAPHA ABBAS[1], MOHAMMED BELLO KAOJE[2], MUKHTAR MOHAMMED[3], MUKHTAR IBRAHIM FURFURI[4], AMINU YUSUF KOKO[5], AMINU MUHAMMAD[6]

[1,2,6]*Department of Physics, Kebbi State University of Science and Technology, Aliero, Nigeria*

[3]*Federal University of Agriculture, Zuru, Kebbi State, Nigeria*

[4]*Federal College of Education Technical, Gusau, Zamfara State, Nigeria*

[5]*Federal University of Education, Kotangora, Niger State, Nigeria*

Abstract- ***The study used the quiet-time geomagnetic field records for the three orthogonal components (H, D and Z) during period of low solar activity year 2017. The quiet field records are uniquely separated into external and internal contributions using the spherical harmonic analysis (SHA) technique. The result shows that the intensity of the external ($MSqH_{ext}$), internal ($MSqH_{int}$), and sum of the quiet field ($MSqH_{Tot}$), equator-ward of the Sq focus are bounded by daytime eastward current which decreases away from the equator and those pole-ward of the Sq focus are bounded by westward current which seems to increases with increasing latitudes. At low latitudes, there was a significant intrusion of the opposite hemisphere summertime external Sq current system into the wintertime hemisphere at pre-noon hours. The ($MSqD_{ext}$), amplitude consistently appeared stronger (weaker) in summer (winter) months reflecting marked effect of ionospheric conductivity caused by solar ionizing flux. The exceptionally large $MSqZ_{ext}$, amplitude at KNY is associated with the reduced and slight phase shift of $MSqH_{ext}$, amplitude at KNY latitude. The result further revealed that the internal Sq focal latitude is consistently more pole-ward that their corresponding external Sq focus which may possibly reflect electromagnetic induction effect.***

Index Terms- ***Ionosphere, Sq current, magnetic field***

I. INTRODUCTION

The ionosphere is a region of the upper atmosphere sandwiched between the magnetosphere and mesosphere. It is composed of partly ionized plasma generated by strong photo-ionization as a result of ionizing solar flux resulting in electrical conductivity of the ionosphere [1]. Based on the ionic configuration, the ionosphere is classified into three distinct layer: the D-layer (innermost layer), E-layer (middle layer) and F-layer (upper layer) respectively. Every day currents are generated through a dynamo mechanism in the E-region of the ionosphere. The basic theory is that prevailing wind system of global scale and solar thermal origin in the E-region of the ionosphere transport conductive plasma across the Earth's main field generating electromotive force (EMF) and established electric field and currents, [2]. The obvious manifestation of the electric current is the apparent signature of geomagnetic daily field variations at the ground surface earlier identified by [3].

On days when solar-terrestrial magnetic disturbances are minimal, the current generated through the dynamo mechanism is called solar quiet current or simply "Sq current" and the associated magnetic field is known as Sq field e.g., [4]. The Sq field shows a smooth regular occurring pattern within a latitudinal range $\sim 60°$S to $60°$N beyond which it is contaminated by auroral activities [5]. It is possible to study the spatial and temporal characteristics of the Sq current by analyzing ground-based magnetic field variations. The Sq current generated in the dynamo E-region of the ionosphere has two current vortices on the dayside. The one in the Northern hemisphere flow counter-clockwise direction and the other flowing in a clockwise direction in the Southern hemisphere [6].

The center of these current vortices is called the Sq current focus.

Studies has shown that Sq current of the upper atmospheric origin penetrate into the conductive Earth structure and the depth extent it can penetrate depends on the effective wavelength of the source current and the conductive properties of the Earth's mantle [7]. The Sq current system at any magnetic observatory has two components. The external component from the dynamo region of the ionosphere and the internal component induced by the external source current [8]. The magnitude of the internally induced Sq current system is half that of the external Sq current [8]. Just like the external Sq current, the internal Sq current system also has two vortices, one flowing clockwise (counter-clockwise) in the northern (Southern) hemispheres which are completely opposite to the external current vortices [9]. The use of spherical harmonic analysis (SHA) allows the separation of the external source field and the internal field below the observation level. On the basis of this [3] used the SHA and separated the Sq fields into their external and internal components and observed that larger part comes from external origin with smaller part from the current induced into the conducting Earth by the external source field. Later, other research workers estimated the external and internal part of the Sq fields e.g., [10].

Ever since the first separation of the Sq fields into their external and internal components, no much work has been done to characterize the external and internal part of the Sq fields possibly due to the complex mathematical procedure required and the lack of spatial distribution of magnetic observatories that are required. Hence, adequate knowledge on the variability of the external and internal Sq fields remains elusive. In this view, we describe in section 2 the source of data and analysis procedure. Presented in section 3 is the result of the analysis and the discussion of the result is presented in section 4. Finally we draw a logical conclusion of this work in section 5.

II. MATERIALS AND METHODS

2.1. Sources of Data

The year 2017 is used to characterize the external, internal and sum (external plus internal) part of the Sq fields. The year (2017) is chosen because it is a low solar activity year with complete data to study the features of the Sq field. To further ensure only quiet days are engaged, only days with $Kp \leq 3$ are used in the analysis as earlier suggested by [11]. These Kp index values were obtained from the World Data Catalogue at: http://wdc.kugi.kyoto-u.ac.jp/. These days have minimal magnetic field disturbance thus makes it suitable to study the variability of the Sq fields. The magnetic field data were obtained from the International Real-time Magnetic Observatory Network (INTERMAG NET) downloaded from the website www.intermagnet.org. To avoid other mechanisms such as auroral electrojet current from affecting the features of the Sq current the geomagnetic stations were limited within ± 60° MLAT as suggested by [12]. Table 1 shows the list of the stations and their magnetic coordinates used in the study.

Table 1 List of INTERMAGNET data stations and their coordinates system used in the study

		Geographic		Geomagnetic
Name	Code	Lat. (°N)	Lon. (°E)	Lat. (°N)
Dalat	DLT	11.94	108.48	2.60
Phuthy	PHU	21.03	105.97	10.78
Kanoya	KNY	31.42	130.88	20.50
B.Ming Tom	BMT	40.30	116.20	30.50
Irkutsk	IRT	52.27	104.45	41.84
Parantuka	PKT	52.97	158.25	46.10
Magadan	MGD	60.06	144.19	53.49

2.2. Method of Data Analysis

As illustrated in the data processing routine of Figure 1, the magnetic field data whose Kp ≤ 3 used in this study consists of 1-minute averages which were binned to hourly values by simply taking average of every sixtieth minute values and this process reduced the data to 24 hourly values of each selected quiet day in the study. This procedure is carried out on each orthogonal component (H, D and Z) and the concept of local time was used in the analysis. The baseline for each component and station was obtained by taking the average of the four hourly values flanking the local midnight. Next we estimate the hourly departures that are approximately equal to the hourly solar quiet (Sq) field for each component.

Next we applied a mirror modeling technique which uses magnetic field values at a particular hemisphere to create a secondary hemisphere that is completely opposite to the primary. During this process, the D and Z-components of the secondary hemisphere are caused to be opposite to the primary hemisphere by simply multiplying the D and Z-components by minus one (-1) and the H-field values in the secondary hemisphere is assumed to be similar to the primary. This process caused the field values of the D and Z-component to be reverse source current relative to the primary hemisphere, [7, 13-15]. The seasonal variation is address by simply shifting the field values for each component by six (6) months in such a way that the summer hemisphere of the primary hemisphere aligned to the winter hemisphere of the secondary hemisphere [7].

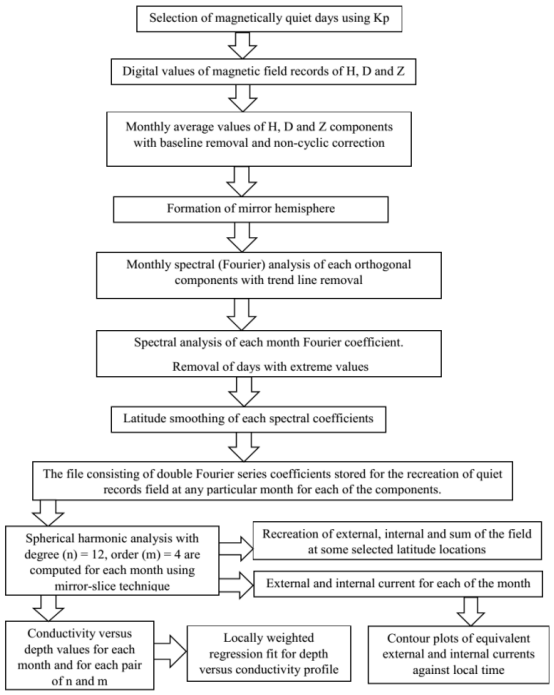

Figure 1 Flow diagram for spherical harmonic analysis of daily Sq field variations

2.2.1Spherical Harmonic Analysis of Solar quiet (Sq)

The next step in the analysis procedure is to represent the field across all the latitudes for any particular time of the year using Fourier cosine and sine harmonic coefficients. Studies have shown that only the spectral contribution to the Sq field at 24-, 12-, 8- and 6-hr harmonics components contribute significantly to the Fourier analysis. These spectral components (24-, 12-, 8-, and 6-hr) are assumed to correspond to the $\left(\frac{360}{m}\right)^{\circ}$ component of longitudinal field changes. As a result of this, the detrended Sq field records are used to determine for each station the 24-, 12-, 8-, and 6-hr monthly Fourier sine and cosine coefficients [7]. The annual and semi-annual Fourier components of 12 (months) daily coefficients in each year were also determined at every 2.5° increment in geomagnetic latitude from the equator [10, 13]. The Fourier coefficients obtained are stored in a separate file and these values represent the Sq field variations for each component.

In SHA, the field components are obtained from magnetic potential function having two converging infinite series of terms, [13, 16]. The magnetic

potential of the quiet field obtained from the daily mean values are from currents of external and internal sources. These magnetic potentials are expressed as;

$$V_n^m = C + a\sum_{n=1}^{\infty}\sum_{m=0}^{n}\left\{\left[a_n^{me}\left(\frac{r}{a}\right)^n + a_n^{mi}\left(\frac{a}{r}\right)^{n+1}\right]\sin(m\phi)\right.$$

$$\left.+\left[b_n^{me}\left(\frac{r}{a}\right)^n + b_n^{mi}\left(\frac{a}{r}\right)^{n+i}\right]\sin(m\phi)\right\}P_n^m(\theta) \qquad 1$$

Where C, θ, a, r and ϕ represent integration constant, geomagnetic colatitude, geocentric distance, Earth's radius and local time of each station. Equation 1 shows that for each $\mathrm{r^n}$ term shows that as n increases the $\mathrm{r^n}$ become larger indication of approaching the external source current responsible for the external field. The second series with $\left(\frac{1}{r}\right)^n$ terms increase as r becomes smaller and smaller indication of approaching the internal current source responsible for the internal field. The a_n^{me}, b_n^{me} and a_n^{mi}, b_n^{mi}parameters represent the Gauss coefficient for the external and internal field sources. During the analysis, it was observed that at a particular n values, there was no significant contribution to the magnetic field as such the spherical harmonic was only conducted on the magnetic function V for order m=1 to m=4 and degree n=m to n=12.

From equation 1, Fourier series provide the longitudinal dependence of the magnetic field potential while the latitudinal dependence is represented by a series of Schmidt quasi-normalized associated Legendre functions P_n^m. These functions are estimated using the following recursive formula as provided in [7];

$$\mathrm{R_n^m} = \sqrt{\mathrm{n^2 - m^2}}$$

2a

$$\mathrm{P_0^0 = 1;\ P_1^0 = (\cos);\ P_1^1 = (\sin\theta)} \qquad 2b$$

$$P_m^m = \sqrt{\frac{2m-1}{2m}}\sin\theta P_{m=1}^{m-1} \text{ for m> 1, n=m} \qquad 2c$$

$$\mathrm{P_n^m = \frac{(2n-1)\cos\theta\ P_{n-1}^m - R_{n-1}^m P_{n-2}^m}{R_n^m}\ for\ n > m} \qquad (2d)$$

$$P_n^m = \frac{(2n-1)\cos\theta P_{n-1}^m - R_n^m P_{n-2}^m}{R_n^m} \text{ (Except for } \theta = 0 \text{ or } 180°)$$

2e

$$\frac{dp_n^m}{d\theta} = \frac{n\cos\theta P_n^m(\cos\theta - R_n^m P_{n-1}^m}{\sin\theta} \qquad 2f$$

The following parameters are used to determine the spherical harmonic Gauss coefficients;

$$a_n^m = \frac{2n+1}{4n(n+1)}\left(\sum_0^{180} x_c^m \frac{dp_n^m}{d\theta}\sin\theta + Y_s^m\, mP_n^m\right)\Delta\theta \qquad 3a$$

3a

$$b_n^m = \frac{2n+1}{4n(n+1)}\left(\sum_0^{180} x_s^m \frac{dp_n^m}{d\theta}\sin\theta + Y_c^m\, mP_n^m\right)\Delta\theta \qquad 3b$$

$$\mathrm{C_n^m = \frac{1}{4}(2n+1)\sum_0^{180} Z_c^m P_n^m \sin\theta\,\Delta\theta} \qquad 3c$$

$$\mathrm{d_n^m = \frac{1}{4}(2n+1)\sum_0^{180} Z_s^m P_n^m \sin\theta\,\Delta\theta} \qquad 3d$$

where X_c^m and X_s^m represent the cosine and sine coefficients of the Fourier component of the ΔH field at colatitude (θ). The $\Delta\theta$ is the step increment which is taken as 2.5^0 $(\Delta\theta = 2.5^{\circ})$ in the analysis. The spherical harmonic Gauss coefficient for the external and internal part is estimated using the following equation;

For the external part;

$$\left.\begin{aligned} \mathrm{a_n^{me}} &= \frac{[(n+1)a_n^m + C_n^m]}{2n+1} \\ \mathrm{b_n^{me}} &= \frac{[(n+1)b_n^m + d_n^m]}{2n+1} \end{aligned}\right\} \qquad 4a$$

The internal part is given as;

$$\left.\begin{aligned} \mathrm{a_n^{mi}} &= \frac{[na_n^m - C_n^m]}{2n+1} \\ \mathrm{b_n^{mi}} &= \frac{[nb_n^m - d_n^m]}{2n+1} \end{aligned}\right\} \qquad 4b$$

The potential function was separated into external and internal source contributions. With reference to Gauss

coefficients, the external fields in the orthogonal directions (X, Y and Z) are reconstructed from the external spherical harmonic analysis as series of Fourier cosine and sine of the terms;

$$X_c^m(\theta) = \sum_{n=m}^{12} a_n^{me} \frac{dP_n^m}{d\theta} \quad 5a$$

$$X_s^m(\theta) = \sum_{n=m}^{12} b_n^{me} \frac{dP_n^m}{d\theta} \quad 5b$$

$$Y_c^m(\theta) = -\frac{m}{\sin\theta} \sum_{n=m}^{12} b_n^{me} \frac{dP_n^m}{d\theta} \quad 5c$$

$$Y_s^m(\theta) = -\frac{m}{\sin\theta} \sum_{n=m}^{12} a_n^{me} \frac{dP_n^m}{d\theta} \quad 5d$$

$$Z_c^m(\theta) = \sum_{n=m}^{12} n a_n^{me} P_n^m \quad 5e$$

$$Z_s^m(\theta) = \sum_{n=m}^{12} n b_n^{me} P_n^m \quad 5f$$

where X_c^m, Y_c^m and Z_c^m represents the cosine coefficients of the external orthogonal field components and X_s^m, Y_s^m and Z_s^m represent the Sine coefficients. For the internal horizontal component X, eastward Y and vertical Z, their fields are reconstructed from the SHA coefficients as series of Fourier cosine and sine terms that are expressed as;

$$X_c^m(\theta) = \sum_{n=m}^{12} a_n^{mi} \frac{dP_n^m}{d\theta}$$

6a

$$X_s^m(\theta) = \sum_{n=m}^{12} b_n^{mi} \frac{dP_n^m}{d\theta} \quad 6b$$

$$Y_c^m(\theta) = -\frac{m}{\sin\theta} \sum_{n=m}^{12} b_n^{mi} \frac{dP_n^m}{d\theta} \quad 6c$$

$$Y_s^m(\theta) = -\frac{m}{\sin\theta} \sum_{n=m}^{12} a_n^{mi} \frac{dP_n^m}{d\theta} \quad 6d$$

$$Z_c^m = \sum_{n=m}^{12} n a_n^{me} P_n^m \quad 6e$$

$$Z_s^m = \sum_{n=m}^{12} n b_n^{me} P_n^m \quad 6f$$

For the vertical component, we use;

$$Z_c^m(\theta) = -\sum_{n=m}^{12} (n+1) a_n^{mi} P_n^m \quad 6g$$

$$Z_s^m(\theta) = -\sum_{n=m}^{12} (n+1) b_n^{mi} P_n^m \quad 6h$$

The sphere in which the spherical harmonic analysis was done was spherically created to accommodate the boundary conditions of the Gauss method. At any particular geomagnetic latitude (90 - θ), any or all of the three orthogonal external or internal field components are obtained from the external and internal SHA coefficients using the following relations;

$$\left.\begin{aligned} X(\theta,\varphi) &= \sum_{m-1}^{4} [X_c^m(\vartheta)\cos(m\varphi) + X_s^m \sin(m\varphi)] \\ X(\theta,\varphi) &= \sum_{m-1}^{4} [Y_c^m(\vartheta)\cos(m\varphi) + Y_s^m \sin(m\varphi)] \\ X(\theta,\varphi) &= \sum_{m-1}^{4} [Z_c^m(\vartheta)\cos(m\varphi) + Z_s^m \sin(m\varphi)] \end{aligned}\right\} \quad (7)$$

III. RESULTS AND DISCUSSION

The magnetic field record during low solar activity year 2017 is used in the study. The external and internal Gauss coefficient obtained from SHA technique allowed for the reconstruction of the monthly Sq field variation for each component (H, D and Z). Figures 2 and 3 displays the monthly external and internal latitudinal Sq field variations reconstructed from the spherical harmonic coefficients. The Sq field provides the variations in the intensity and phase of both the external and internal induced current.

It is obvious from Figure 2 that the external horizontal (H) field is characterized by a negative night-time (17:00-05:00 LT) hrs variations that are apparent at the latitudes of DLT, PHU and oscillate at KNY latitudes. At latitude beyond KNY, the $MSqH_{ext}$ exhibit positive night-time amplitudes that extended to the MGD latitude (see Figure 2 panel H2). The internal horizontal field component $MSqH_{int}$ also exhibit similar negative night-time amplitudes at DLT, PHU and KNY and thereafter turned positively enhanced as depicted in Figure 3 (panel H5).

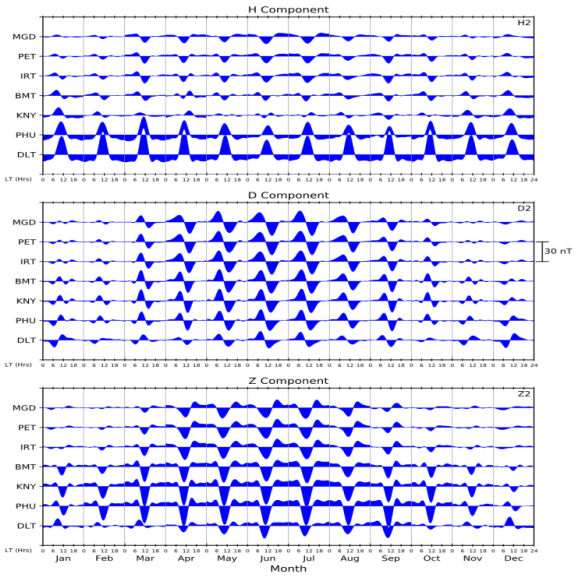

Figure 2 Monthly external field variations of the H, D, and Z reconstructed from the spherical harmonic coefficients

The night-time (17:00-05:00 LT) hrs negative $MSqH_{ext}$ and $MSqH_{int}$ amplitudes at DLT, PHU and later extended to KNY depict a well-defined presence of westward current consistent with the night-time Sq current distributions earlier established by [17-18].

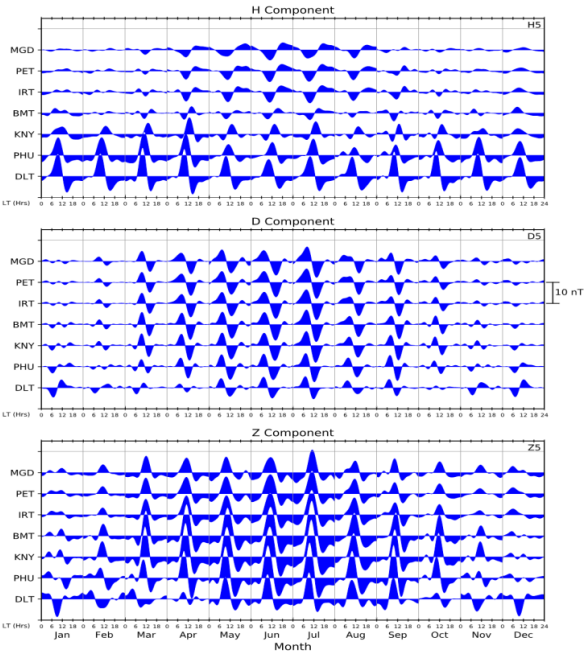

Figure 3 Monthly internal field variations of the three orthogonal components (H, D, and Z) reconstructed from the spherical harmonic coefficients.

These authors pointed out that the Sq current and associated electric field reverse their direction and flow westward at night-time. The daytime (06:00-16:00 LT) hrs, $MSqH_{ext}$ amplitudes are positively enhanced at DLT and PHU with a significant reduction that is associated with a slight phase shift at KNY and thereafter changed to negative $MSqH_{ext}$ amplitude. The reduced $MSqH_{ext}$ magnitude with a slight phase change suggests likely presence of the external Sq focus nearer to KNY latitude. Similarly, the marked reduction in $MSqH_{int}$ amplitudes at BMT latitude and the subsequent changeover variation pattern pole-ward of BMT suggest likely position of the internal Sq current focus nearer to BMT latitude as shown in Figure 3 (panel H5). These results confirmed that the internal Sq current focus is relatively pole-ward than their corresponding external focus. The latitudinal difference in the position of the external and internal Sq focus may be attributed to the local conductivity effect, [13].

During these periods, the daytime positive and negative $MSqH_{ext}$ amplitude ~40 and -15 nT occurred in March and February at DLT and MGD around 10:00 and 12:00 LT indication of stronger solar ionizing flux (see Figure 2, panel H2). Similarly, daytime positive $MSqH_{int}$ are seen at DLT, PHU and KNY latitudes and thereafter change to negative variations as seen in Figure 2 (panel H2). The daytime positive $MSqH_{int}$ amplitudes reached ~13 nT around 10:00 LT hrs in March at DLT. The greater daytime $MSqH_{ext}$ and $MSqH_{int}$ magnitudes with their higher intensity between 10:00 LT and 13:00 LT hrs demonstrate the evidence of stronger Sq current caused by intense ionospheric conductivity under the influence strong dynamo action around these periods. The monthly diurnal variation shows that the $MSqH_{ext}$ amplitudes are about twice lager than their corresponding $MSqH_{int}$ amplitudes. Their greater magnitude reflects direct effect of solar ionizing flux. On the other hand, $MSqH_{int}$ reflect most of the features of the $MSqH_{ext}$ but are more variable which may likely be affected by geological condition of the study area.

Figure 2 (panel D2) illustrate the external field variation of the eastward (D) component $MSqD_{ext}$. As can be observed from the Figure, the $MSqD_{ext}$ show a pre-noon positive amplitude between 01:00 and 11:00 LT hrs and changed to negative amplitude between

12:00 and 18:00 LT hrs seen during the summer and equinoctial months (March-October). The pre-noon (afternoon) positive (negative) $MSqD_{ext}$ in summer and equinoctial months (April-September) suggest a well-define southward (northward) currents consistent with the northern stations [19]. During these periods, the maximum pre-noon amplitude reached ~25 nT around 08:00 LT hrs in May at KNY and its afternoon magnitude ~30 nT occurred around 13:00 LT hrs in June at MGD respectively. Seasonally, $MSqD_{ext}$ amplitudes appeared stronger (weaker) in summer (winter) months. Similar positive (negative) $MSqD_{int}$ amplitudes are seen during the pre-noon (afternoon) in summer and equinoctial months. The pre-noon positive amplitude reached ~ 8 nT around 06:00 LT at MGD in May (see Figure 2 panel D2) and its afternoon negative amplitude reached ~-9 nT in May around 13:00 LT at MGD.

Strange positive $MSqD_{ext}$ amplitudes are seen between 16:00 and 1800 LT hrs that are more prominent at IRT, BMT and KNY in November-February suggest likely effect of the field-aligned current that appears weak during the dusk sector [20]. The additional negative $MSqD_{ext}$ amplitude during the dawn sector (0500-0700 LT) hrs in March and October across the latitudes may be associated to the field aligned currents (FACs). The present study for the first time (to the best of our knowledge) identify $MSqD_{ext}$ amplitudes with "W shape" form of variations seen across all the latitudes exception of DLT in northern winter months (November-February) as shown in Figure 1 (panel D2). Traces of "W shape" are also eminent in $MSqD_{int}$ amplitudes as shown in Figure 3 (panel D5). These variations pattern indicate disturbances of the north-south component of the meridional current system. The variation pattern of $MSqD_{ext}$ at DLT in winter months shows absence of prominent southward (northward) flow of Sq current system consistent with the pre-noon (afternoon) periods rather a northward (southward) current flow is seen at these latitudes. The $MSqD_{ext}$ variations patterns are contrary to the stations located in the northern hemisphere and thus suggest possible intrusion of other currents system.

Figure 2 (panel Z2) illustrate the external quiet field of the vertical Z-component $MSqZ_{ext}$ reconstructed from the SHA coefficients. It is obvious from Figure 2 (panel Z2) that $MSqZ_{ext}$ showed night-time (17:00-05:00 LT) hrs positive amplitudes and became negative during the daytime (06:00-16:00 LT) hrs exception of DLT that exhibit daytime positive $MSqZ_{ext}$ amplitudes. These variation patterns are expected of stations located in the northern hemisphere. During these periods, $MSqZ_{ext}$ reached ~33 nT around 11:00 LT hrs at PHU in September (see Figure 2 panel Z2). The amplitude of $MSqZ_{ext}$ appeared weaker at DLT located closer to the magnetic equator, became stronger at mid-latitude and decreases significantly with increasing latitudes. The sharp decrease of both $MSqZ_{ext}$ and its corresponding $MSqZ_{int}$ amplitudes are consistent with the Chapman's theory that the field decreases and become zero (flat) at the magnetic equator. Since DLT is not exactly at dip equator but lie somewhere at the equatorial latitude suffered reduced magnitudes. The $MSqZ_{int}$ exhibits opposite polarity to the $MSqZ_{ext}$. Throughout the year, the magnitudes of $MSqZ_{ext}$ were about twice larger than their corresponding $MSqZ_{int}$ magnitudes.

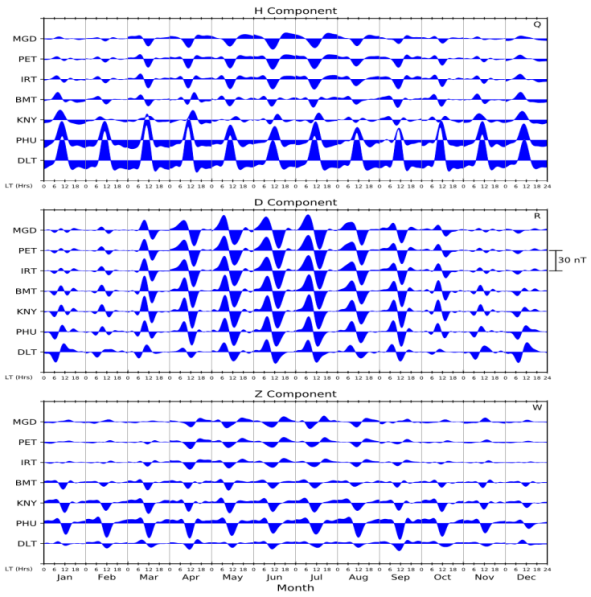

Figure 4 Sum of the quiet monthly field variations reconstructed from the spherical harmonic coefficients.

Figure 4 illustrate the sum (external plus internal) of the Sq field reconstructed from SHA for each component (H, D and Z). The Figure revealed that the sum of the H-component $MSqH_{Tot}$ is characterized by semi-annual variation with night-time (17:00-05:00

LT) hrs negative amplitudes and daytime positive amplitudes at the DLT and PHU latitudes and significantly decrease at KNY latitude (see Figure 4 panel Q). The $MSqH_{Tot}$ amplitude reached ~53 nT in March seen around 11:00 LT hrs at DLT depicting the effect of solar activity in modulating the ionospheric conductivity. The $MSqH_{Tot}$ magnitudes generally appear higher at low latitudes (DLT and PHY) decrease at KNY and thereafter reverse its polarity. The significant decrease and phase shift of $MSqH_{Tot}$ at PHU and the dramatic change from daytime eastward to westward field at KNY latitude suggest possible position of the sum of Sq current focus between PHU and KNY latitudes.

The magnitudes of $MSqH_{Tot}$ are greater in summer and equinoctial months and weaker in winter months. The sum of the quiet eastward D-component $MSqD_{Tot}$ exhibit a well-defined maximum pre-noon (afternoon) positive (negative) amplitude reached ~27 nT (~-29 nT) in May (June) as shown in Figure 4 (panel R). Throughout the year the $MSqD_{Tot}$ magnitude has not shown significant changes indication of lesser influence of solar activity on the $MSqD_{Tot}$ magnitudes. The sum of the vertical field component $MSqZ_{Tot}$ is shown in Figure 4 (panel W). The $MSqZ_{Tot}$ showed less variable night-time (16:00-05:00 LT) hrs positive amplitude in most cases and a daytime (09:00-15:00 LT) hrs negative amplitudes (see Figure 4 panel W). During these periods, the highest daytime negative $MSqZ_{Tot}$ amplitude ~ 28 nT occurred around 11:00 LT at PHU in September.

CONCLUSION

In this study, we describe the monthly behavior of both the external, internal and sum (external plus internal) quiet magnetic fields derived from the spherical harmonic analysis coefficients during the low solar activity year 2017. The main findings from the study are summarized as follows:

1. The study has effectively demonstrated that the internal Sq focus consistently appeared pole- ward relative to the external focus. The latitudinal difference in the position of the external and internal Sq focus may be attributed to electromagnetic induction effect.
2. The daytime positive $MSqH_{ext.}$and $MSqH_{int}$ amplitudes of stations equator-ward (pole-ward) of the Sq focus decreases (increases) with increasing latitudes
3. The daytime Higher MSqHext magnitudes between 10:00 and 13:00 LT hrs reflect direct effect of stronger Sq current caused by stronger ionospheric conductivity under the influence intense solar activity.
4. Both $MSqD_{ext}$ and $MSqD_{int}$ amplitudes are consistently stronger (weaker) in summer (winter) months reflecting differences in the source and driving mechanisms.
5. Generally the external field variations are about twice greater than the internal field for the orthogonal field element.
6. The $MSqD_{ext}$ and $MSqD_{int}$ 'W shape' identified for the first time in the present study indicates disturbance effect on the meriodional current system.
7. The strange positive MSqDext amplitudes between 16:00 and 18:00 LT hrs suggest likely modification of the meridional current system.
8. The $MSqZ_{ext}$ appeared exceptionally large at KNY latitude nearer to the Sq focus permitting an inference that the reduction in the intensity of $MSqH_{ext}$ at KNY latitude cause incredible enhancement on the form of $MSqZ_{ext}$ amplitude.

ACKNOWLEDGMENTS

We thank the institutions and INTERMAGNET team for promoting high quality data used in this study. We also extend gratitude to the World Data Centre Kyushu, Japan for providing the Kp indices used in the study.

REFERENCES

[1] Abbas M, Abidin ZZ, Jusoh MH, Bolaji OS, Yoshikawa A. Features of horizontal magnetic field intensity over northern island of Malaysia. Indian Journal of Physics. 2019 , Oct; 93 (10):1247-57.

[2] Pedatella NM, Forbes JM, Richmond AD. Seasonal and longitudinal variations of the solar quiet (Sq) current system during solar minimum determined by CHAMP satellite magnetic field observations. Journal of Geophysical Research: Space Physics. 2011 Apr;116(A4).

[3] Schuster, A. (1907). The diurnal variation of terrestrial magnetism. *Proc. R. Soc. Lond. A*, *80*(535), 80-82.

[4] Xu, W.Y. and Li, W. D. Longitudinal effects and UT variations of the geomagnetic Sq Field. Chinese Journal of Geophysics, 37, 440-447. https:// doi.Org /10.1029/2002JA009287.

[5] Vichare, G., Rawat, R., Jadhav, M., & Sinha, A. K. (2017). Seasonal variation of the Sq focus position during 2006–2010. *Advances in Space Research, 59*(2), 542-556.

[6] Yamazaki Y, Maute A. Sq and EEJ—a review on the daily variation of the geomagnetic field caused by ionospheric dynamo currents. Space Science Reviews. 2017 Mar;206(1):299-405.

[7] Campbell WH. Introduction to geomagnetic fields. Cambridge University Press; 2003 Apr 10.

[8] Liu, Xiaocan, Peng Han, Katsumi Hattori, Huaran Chen, Junjie Chen, Liguo Jiao, Jiyao Tu, Yu Lei, and Junhao Zhao. "Seasonal variations of Sq current system in different longitudinal sectors and solar activities." *Journal of Geophysical Research: Space Physics* 129, no. 1 (2024): e2023JA031956.

[9] Liu, Xiaocan, Peng Han, Katsumi Hattori, Huaran Chen, Chie Yoshino, Xudong Zhao, Liguo Jiao, Xinxin Ma, and Yu Lei. "Seasonal variation characteristics of geomagnetic Sq external and internal equivalent current systems in East-Asia and Oceania regions." *Journal of Geophysical Research: Space Physics* 126, no. 3 (2021): e2021JA029113.

[10] Campbell, W. H., & Schiffmacher, E. R. (1987). Quiet ionospheric currents and earth conductivity profile computed from quiet-time geomagnetic field changes in the region of Australia. *Australian journal of physics*

[11] Campbell, W. H. (2003). *Introduction to geomagnetic fields*: Cambridge University Press.

[12] Matsushita, S., & Maeda, H. (1965). On the geomagnetic solar quiet daily variation field during the IGY. *Journal of Geophysical Research, 70*(11), 2535-2558.

[13] Campbell WH, Schiffmacher ER. Upper mantle electrical conductivity for seven subcontinental regions of the Earth. Journal of geomagnetism and geoelectricity. 1988;40(11):1387-406.

[14] WH C, CE B, FH C. Quiet-day ionospheric currents and their application to upper mantle conductivity in Australia. Earth, planets and space. 1998;50(4):347-60.

[15] Campbell W H. Differences in geomagnetic Sq field representations due to variations in spherical harmonic analysis techniques. Journal of Geophysical Research: Space Physics. 1990 Dec 1;95(A12):20923-36.

[16] Campbell WH. The regular geomagnetic field variations during quiet solar conditions. Geomagnetism. 1989;3:385-460.

[17] Takeda M, Araki T. Electric conductivity of the ionosphere and nocturnal currents. Journal of atmospheric and terrestrial physics. 1985 Jun 1;47(6):601-9.

[18] Stening R J, and Winch D. E. Night-time geomagnetic variations at low latitudes. Planetary and space science. 1987 Dec 1;35(12):1523-39.

[19] Stening RJ, Winch DE. The ionospheric Sq current system obtained by spherical harmonic analysis. Journal of Geophysical Research: Space Physics. 2013 Mar; 118(3):1288-97.

[20] Stening, R. J. Variations in the strength of the Sq current system. Annales Geophysicae, 13, 627-632. https://doi.org/10.1007/s00585-995-0627-5.